

# Polarization dependence of non-linear gain compression factor in semiconductor optical amplifier

Severine Philippe<sup>1</sup>, A. Louise Bradley<sup>1</sup>, Ramon Maldonado-Basilio<sup>2,3</sup>, Frederic Surre<sup>1,2</sup>,  
Brendan F. Kennedy<sup>2,4</sup>, Pascal Landais<sup>2\*</sup> and Horacio Soto-Ortiz<sup>3</sup>

<sup>1</sup>*School of Physics, Trinity College Dublin, Dublin 2, Ireland*

<sup>2</sup>*School of Electronics Engineering, Dublin City University, Dublin 9, Ireland*

<sup>3</sup>*CICESE Research Center, Applied Physics Division, Carretera Tijuana-Ensenada, Ensenada 22860, Baja California, Mexico*

<sup>4</sup>*Electrical Engineering Department, Universidad de Santiago de Chile, Avda. Ecuador 3519, Estacion Central, Santiago, Chile.*

\*Corresponding author: [landaisp@eeng.dcu.ie](mailto:landaisp@eeng.dcu.ie)

**Abstract:** We investigate the power and the polarization dependence of the intraband dynamics in a bulk semiconductor optical amplifier using both a 2.5-ps pump-probe experimental set-up in contra-propagation and a theoretical model. Our model is based on the rate equations and takes into account the polarization dependence of the gain. By comparing experimental and computational results we are able to highlight the dependences of the intraband dynamics and to extract the non-linear gain compression factor as a function of both pulse energy and polarization of the injected pulses.

©2008 Optical Society of America

**OCIS codes:** (250.5980) Optoelectronics. Semiconductor Optical Amplifier; (260.5430) Physical Optics. Polarization

---

## References and links

1. L. Occhi, Y. Ito, H. Kawaguchi, L. Schares, J. Eckner, and G. Guekos, "Intraband gain dynamics in bulk semiconductor optical amplifiers: measurements and simulations," *IEEE J. Quantum Electron.* **38**, 54-60 (2002).
2. P. Borri, W. Langbein, J. Mørk, J. M. Hvam, "Heterodyne pump-probe and four-wave mixing in semiconductor amplifiers using balanced lock-in detection," *Opt. Commun.* **169**, 317-324 (1999).
3. A. Mecozzi and J. Mørk, "Saturation effects in nondegenerate four-wave mixing between short optical pulses in semiconductor laser amplifiers," *IEEE J. Sel. Top. Quantum Electron.* **3**, 1190-1207 (1997).
4. F. Girardin, G.H. Duan, P. Gallion, "Linewidth rebroadening due to nonlinear gain and index induced by carrier heating in strained quantum-well lasers," *IEEE Photon. Technol. Lett.* **8**, 334-336 (1996).
5. G. P. Agrawal and N. A. Olsson, "Self-phase modulation and spectral broadening of optical pulses in semiconductor laser amplifiers," *IEEE J. Quantum Electron.* **25**, 2297-2306 (1989).
6. S. Philippe, A.L. Bradley, B.Kennedy, F.Surre, P.Landais, "Experimental investigation of polarization effects in semiconductor optical amplifiers and implications for all-optical switching," *J. Lightwave Technol.* (to be published).
7. N. A. Olsson and G. P. Agrawal, "Spectral shift and distortion due to self-phase modulation of picosecond pulses in 1.5  $\mu$  m optical amplifiers," *Appl. Phys. Lett.* **55**, 13-15 (1989).
8. M. Y. Hong, Y. H. Chang, A. Dienes, J. P. Heritage, P. J. Delfyett, "Subpicosecond pulse amplification in semiconductor laser amplifiers: theory and experiment," *IEEE J. Quantum Electron.* **30**, 1122-1131 (1994).
9. M. Y. Hong, Y. H. Chang, A. Dienes, J. P. Heritage, P. J. Delfyett, S. Dijaili, F. G. Patterson, "Femtosecond self- and cross-phase modulation in semiconductor laser amplifiers," *IEEE J. Sel. Top. Quantum Electron.* **2**, 523-539 (1996).
10. W. Wang, K. Allaart, D. Lenstra, "Semiconductor optical amplifier gain anisotropy: confinement factor against material gain," *Electron. Lett.* **4**, 1602-1603 (2004).
11. B. F. Kennedy, S. Philippe, P. Landais, A.L. Bradley, H. Soto-Ortiz, "Experimental investigation of polarization rotation in semiconductor optical amplifiers," *IEEE Proc.-Optoelectron.* **151**, 114-118 (2004).
12. R. Gutierrez-Castrejon, L. Schares, L. Occhi, G. Guekos, "Modeling and measurement of longitudinal gain dynamics in saturated semiconductor optical amplifiers of different length," *IEEE J. Quantum Electron.* **36**, 1474-1484 (2000).

13. E. Alvarez, H. Soto, J. Torres, "Investigation of the carrier density dependence on the confinement factor in a bulk semiconductor optical amplifier with a ridge waveguide," *Opt. Commun.* **222**, 161-167 (2003).
  14. H. Soto, E. Álvarez, C. A. Díaz, J. Topomondzo, D. Erasme, L. Schares, L. Occhi, G. Guekos, M. Castro, "Design of an all-optical NOT XOR gate based on cross-polarization modulation in a semiconductor optical amplifier," *Opt. Commun.* **237**, 121-131 (2004).
  15. A. Uskov, J. Mørk, J. Mark, "Wave mixing in semiconductor optical amplifiers due to carrier heating and spectral-hole burning," *IEEE J. Quantum Electron.* **30**, 1769-1781 (1994).
  16. T. Durhuus, B. Mikkelsen, K.E. Stubkjaer, "Detailed dynamic model for semiconductor optical amplifiers and their crosstalk and intermodulation distortion," *J. Lightwave Technol.* **10**, 1056-1065 (1992).
- 

## 1. Introduction

As data bit-rates increase, intraband effects like carrier heating (CH) and spectral hole burning (SHB) in semiconductor materials have a greater influence on optical signal generation and propagation. For example, a bit rate of 40Gb/s corresponds to pulsewidths of 8ps. And for higher bit rates the pulsewidth will be even smaller. As CH has a timescale of up to 2ps [1], it is not possible anymore to neglect intraband effects for such short pulses.

The necessity to take intraband effects into accounts leads to the problem of how to model them for SOA design purpose. A simple and efficient approach is to add a non-linear gain compression correction factor,  $\epsilon$ , in the expression of the gain. It is widely used to take into account intraband non-linearities in the mechanisms of gain recovery in semiconductor devices. Even if this approach has proven its worth for lasers, the largest extracted value from experimental results is more than 10 times larger than the smallest extracted value [1-4].

By using a contra-propagation pump-probe set-up described in Section 2 and a phenomenological model including the non-linear gain compression factor  $\epsilon$ , it is possible to study the influence of the polarization of the optical pulses on the extracted values of  $\epsilon$ . The model is derived from previous work by Agrawal *et al.* [5]. The modifications are concerned with the introduction of TE and TM polarization and the inclusion of the non-linear gain compression correction factor into the gain expression, cf. Section 3. The study of the influence of the polarization shows that the value of  $\epsilon$  is greatly dependent on the state of polarization of the injected signals. This is described in Section 4, where the influence of the pulse energy is also presented.

## 2. Experimental setup

The device under test is a commercially available 1.5 mm long bulk InGaAsP/InP traveling wave SOA. It is biased at 350 mA and temperature regulated at 20°C by means of a Peltier cooler. Under these experimental conditions, the gain peak is at 1580 nm and the material gain along the TM axis is slightly larger than in TE by about 1dB.

Although a more complicated co-propagation heterodyne detection technique [2] has been proposed, a simpler and more flexible method to study the polarization dependence of pump-probe measurements is to use a contra-propagation configuration where the pump and probe pulses travel in opposite directions. Then, the signals can simply be separated using a beam-splitter, whatever their state of polarization or wavelength may be. The analysis and modeling of the experimental data is not straightforward since the probe experiences different gain recovery processes as it travels through the SOA. For one pump probe delay, part of the SOA could be saturated by the pump signal while another section could already have recovered mainly by intraband effects. It is important to note that the drawbacks of contra-propagation set-up (longer fall time, pulses overlapping at different places inside the SOA depending on the delay) are not relevant here as the proposed model will take them into account, allowing an estimate of  $\epsilon$  comparable to that achieved in a co-propagation set-up. A schematic and a full description of the set-up can be found in [6]. It is a one color pump probe contra-propagation set-up with a full control of the state of polarization of the pump and probe signals injected. The wavelength of both 2.5ps injected pulses is 1580nm, corresponding to the gain peak.

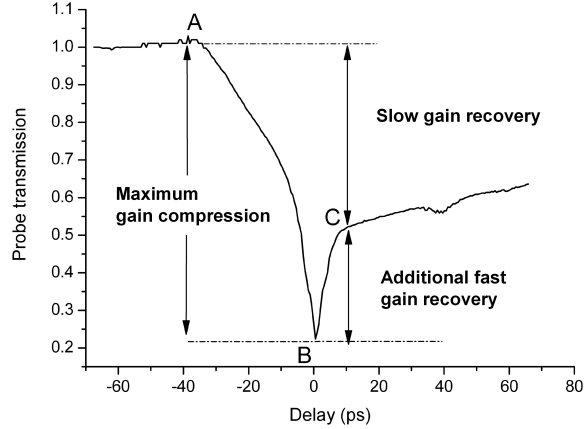


Fig. 1 Main features of a transmission curve.

A typical probe intensity signal transmission obtained in contra-propagation is shown in Fig. 1. The output signal, proportional to the probe intensity, is normalized by the probe signal level that is achieved in the absence of the pump pulse in order to give transmission values. As discussed above, there is not a single value of time delay ( $t = 0$ ) when the pump and probe overlap, rather the position of the pump and probe pulses overlap within the device changes as a function of time delay. Therefore, the relative time delay is set to zero when the influence of the pump is the greatest. We refer to the probe input facet (pump output facet) as the SOA input and the probe output facet (pump input facet) as the SOA output. Before *A*, the probe leaves the SOA before the pump enters it and its transmission is left unchanged. Between *A* and *B* the pulses overlap inside the SOA, the probe gain, averaged over the length of the device, is reduced. Toward the SOA output, the gain has started to recover mainly through intraband processes, however, close to the SOA input, the gain is reduced and eventually saturated. A minimum is reached at *B*, where the pulses overlap at the input of the SOA. This minimum can be expected, as it is at this delay that the pump has affected the entire gain along the SOA structure, with no time for any recovery in the region close to the SOA input. After *B* the pump leaves the SOA before the probe enters it and the gain has started to recover before the arrival of the probe. As the delay is further increased, the amplified probe signal will continue to increase and the recovery time of the device is monitored. Two components can be seen in the recovery of the probe transmission at positive delays. A fast component between *B* and *C*, corresponding to the recovery of the gain compression due to CH and SHB by intraband carrier recombination, and a slower recovery after *C* associated with interband recombination [1]. Even though the timescales for CH and SHB effects cannot be resolved within the time resolution of the 2.5 ps pulses, the polarization dependence of the intraband dynamics can be determined by examining the relative contributions of the fast component to the probe transmission recovery as a function of the delay.

### 3. Theoretical model

#### 3.1 General view

A model based on [5] and [7] has been developed in order to describe the probe transmission dynamics. It is an integration of the first order time derivation of the dynamic saturation of the gain [5]. This integration takes into account the time variation of the electric field of both the pump and the probe. The set of differential equations describing the propagation of a pulse inside the SOA can be found as:

$$\frac{\partial P}{\partial z} = (g - \alpha_{\text{int}})P \quad (1)$$

$$\frac{\partial \phi}{\partial z} = -\frac{1}{2} \alpha g \quad (2)$$

$$\frac{\partial g}{\partial \tau} = \frac{g - g_o}{\tau_c} - \frac{g |A(t)|^2}{E_{sat}} \quad (3)$$

where  $P$  and  $\phi$  are the power and the phase of the pulse respectively,  $\tau = t - z/v_g$  defines a reference frame moving with the pulse at a group velocity  $v_g$ ,  $A$  is the sum of the amplitude of the envelope of the pump and probe pulses propagating in the SOA,  $\tau_c$  is the spontaneous carrier lifetime,  $\alpha_{int}$  corresponds to the internal losses,  $\alpha$  is the linewidth enhancement factor,  $z$  is the longitudinal coordinate,  $E_{sat}$  is the saturation energy,  $g_o$  corresponds to the small signal gain and  $g$  is the material gain defined by:

$$g(N) = \Gamma a(N - N_0) \quad (4)$$

where  $\Gamma$  is the confinement factor,  $a$  the differential gain taking into account intraband effects,  $N$  is the carrier density and  $N_0$  the carrier density at transparency. The model is self-contained with the set of equations (1)-(4), fully describing the propagation of two contra-propagating arbitrary pulses inside a SOA.

### 3.2 Gaussian pulse solutions

If it is assumed that  $g \gg \alpha_{int}$  and the pulses injected are Gaussian, then Eqns. (1)-(3) can be solved analytically as follows:

$$P_{out}(\tau) = P_{in}(\tau) \exp[h(\tau)] \quad (5)$$

$$\phi_{out}(\tau) = \phi_{in} - \frac{1}{2} \alpha h(\tau) \quad (6)$$

$$\frac{\partial h}{\partial \tau} = \frac{g_o L - h}{\tau_c} - \frac{P_{in}(\tau)}{E_{sat}} [\exp(h(\tau)) - 1] \quad (7)$$

$h$  is the gain integrated at each point of the pulse profile. If the pulse width  $\tau_p$  is smaller than the carrier lifetime the first term at the right hand side of Eq. (7) can be neglected. Physically, this means that the pulse is so short that the gain is not able to recover within the timescale of the pulse. This implies that the carrier injection and recombination can be ignored during the passage of the pulse. In these conditions, the solution of (7) is written as:

$$h(\tau) = -\ln\left[1 - \left(1 - \frac{1}{G_o}\right) \exp\left(-\frac{U_{in}(\tau)}{E_{sat}}\right)\right] \quad (8)$$

where  $G_o = \exp(g_o L)$  is the unsaturated single-pass amplifier gain and  $U_{in}$  the fraction of the pulse energy contained in the leading part of the pulse up to  $\tau$  is given by:

$$U_{in}(\tau) = \int_{-\infty}^{\tau} P_{in}(\tau') d\tau' \quad (9)$$

By definition,  $U_{in}(\infty)$  is equal to  $E_{in}$ , the input pulse energy. In the case of an input Gaussian pulse, the instantaneous amplifier gain  $G$  is given by [5]:

$$G(\tau) = \frac{1}{1 - \left(1 - \frac{1}{G_o}\right) \exp\left(-\frac{U_{in}(\tau)}{E_{sat}}\right)} \quad (10)$$

### 3.3 Gain modification

It has been shown that Eqns. (6) and (7) give accurate results for input Gaussian pulses in the range of tens and hundreds of picoseconds. However, for pulses of the order of 1 ps, a semi-classical model has been developed by Hong *et al.* [8] and [9], where the fast dynamics of a SOA, specifically the SHB is included by using a modified gain,  $\bar{g}$ , defined by:

$$\bar{g}(\tau) = \frac{g(\tau)}{f(\tau)} \quad (11)$$

where  $g$  is the material gain given by Eq. (4) and  $f$  the correction factor [8].  $f$  can be expressed as a function of the non-linear gain compression factor,  $\varepsilon$ , by:

$$f(\tau) = 1 + \varepsilon S(\tau) \quad (12)$$

where  $S(\tau)$  is the total photon density generated by the saturating pump pulse signal. Taking into account this modification (12), the set of equations (5)-(7), along with Eq. (10), gives a phenomenological model that allows us to analyze the propagation of a Gaussian pulse in a semiconductor optical amplifier, in a weak or a saturation regime, and with a pulse width longer than 200 fs [8]. This model takes into account the fast gain recovery resulting from the intraband dynamics. However, it does not take into account the slow gain recovery, therefore no variation of the transmission will be present after point *C* as illustrated in Fig. 1. It is also assumed that the pump pulse induces amplifier saturation, which will be of different strength for each of the two waveguide eigen-axes based on the experimentally observed probe transmission curves, shown in Fig. 2(a).

Therefore, in the co-polarized case, the same correction factor and the same saturation energy are used for both pump and probe signals. Derived from Eqns. (10) and (12), the single-pass gain for both pump and probe signal is given by:

$$G^i(\tau) = \frac{1}{1 - (1 - \frac{1}{G_0^i}) \exp(-\frac{U_{in}(\tau)}{E_{sat}^i})} \quad (13)$$

and the correction factor is:

$$f^i(\tau) = 1 + \varepsilon^i S(\tau) \quad (14)$$

where  $i$  corresponds to either TE or TM polarization.

For the cross-polarized case, the pump and probe pulses are propagating along different waveguide eigen-axes. The pump single pass gain and correction factor are given by Eqns (13) and (14). The probe single-pass gain and non-linear correction factor are given by:

$$G_{probe}^{i_{pr}, j_{pu}}(\tau) = \frac{1}{1 - (1 - \frac{1}{G_0^j}) \exp(-\frac{U_{in}(\tau)}{E_{sat}^{i_{pr}, j_{pu}}})} \quad (15)$$

and

$$f_{probe}^{i_{pr}, j_{pu}}(\tau) = 1 + \varepsilon^{i_{pr}, j_{pu}} S(\tau) \quad (16)$$

where  $i$  is the index of the probe polarization and  $j$  the index of the pump polarization, with  $i_{pr}$ ,  $i_{pu}$  either  $TM_{pr}TE_{pu}$  or  $TE_{pr}TM_{pu}$ . In Eqns. (15) and (16) it has been considered that: i) the probe propagation along the crossed eigen-axis experiences an unsaturated gain, and ii) the influence of the pump over the probe appears through coupling terms  $E_{sat}^{i_{pr}, j_{pu}}$  and  $\varepsilon^{i_{pr}, j_{pu}}$ . In this way, the term  $E_{sat}^{i_{pr}, j_{pu}}$  is a measure of the slow gain recovery behavior, related to the slow

gain compression, whilst the term  $\varepsilon^{i_{pr}, j_{pu}}$  is a measure of the saturation strength related to the maximum gain compression. The difference in the values obtained for the carrier density at transparency for the two eigen-axis are in agreement with the ones reported in the literature [10]. The carrier density at transparency for the TM eigen-axis is larger than the one for the TE. The parameters used in this simulation are listed in Table 1.

Table 1. Values of parameters used for the simulations. The carrier densities at transparency and differential gains were calculated from the experimentally determined single pass gain spectra previously reported in [11].

Parameters	Value	Parameters	Value
Length of the active region, $L$	1.5 mm	Carrier density at transparency TE, $N_0^{TM}$	$0.9 \times 10^{24} \text{ m}^{-3}$
Depth of active region, $d$	250 nm	Carrier lifetime, $\tau$	400 ps
Width of active region, $w$	2.2 $\mu\text{m}$	Differential gain TE, $a^{TE}$	$4.38 \times 10^{-20} \text{ m}^2$
Confinement factor TE, $\Gamma^{TE}$	0.43 [12], [13]	Differential gain TM, $a^{TM}$	$6.3 \times 10^{-20} \text{ m}^2$
Confinement factor TM, $\Gamma^{TM}$	0.38 [14]	Single pass gain TE, $G_0^{TE}$	24 dB
Group index TE, $n_g^{TE}$	3.56 [15]	Single pass gain TM, $G_0^{TM}$	25 dB
Group index TM, $n_g^{TM}$	3.52 [16]	Bias current, $I$	350 mA
Carrier density at transparency TE, $N_0^{TE}$	$0.86 \times 10^{24} \text{ m}^{-3}$	Wavelength of pump and probe beams, $\lambda_p$	1580 nm

#### 4. Experimental and simulation results

In this Section, a comparison between the experimental data and the simulation results is presented. The value of  $\varepsilon$  is extracted for each polarization combination. Finally, the influence of the pump pulse energy on the value of  $\varepsilon$  is investigated.

##### 4.1 Polarization dependence of $\varepsilon$

Figure 2(a) shows the experimental results for the transmission of the probe as a function of time delay for co- and cross-polarization cases. The input pump energy is set at 24 fJ and the input probe energy at 12 fJ, well below the saturation energy of this device measured at 40 fJ in the TE case. Due to stimulated emission, the pump pulse is amplified progressively as it propagates through the SOA and this impacts on the transmitted probe signal. As can be seen in Fig. 2(a), the onset of the decrease in the probe transmission occurs at earlier time delays for the co-polarized pump and probe pulses due to the fact that the effect of the pump is greater and therefore it has to traverse less of the SOA length to induce gain compression of the probe signal. An additional feature is observed around -30 ps delay when the pump and probe pulses overlap close to the output facet of the SOA. It can also be noted that this feature is strongly polarization dependent. This feature is most likely due to modification of the carrier distribution along the device, depletion of carriers at a given position inside the device can lead to a decrease of ASE travelling from that position and this increase the carrier density at other position along the SOA.

The total gain compression is measured between  $A$  and  $B$ , cf. Fig. 1. The maximum gain compression is achieved by pumping and probing along the same eigen axis. Along the TM axis, a gain compression of  $\sim 7$  dB is achieved while, for the TE axis, a gain compression of  $\sim 3$  dB. When the probe and the pump are cross-polarized, a lower probe gain compression is observed. In the  $\text{TE}_{pr}\text{TM}_{pu}$  configuration the gain compression is  $\sim 0.7$  dB while in  $\text{TM}_{pr}\text{TE}_{pu}$  it is  $\sim 1.2$  dB.

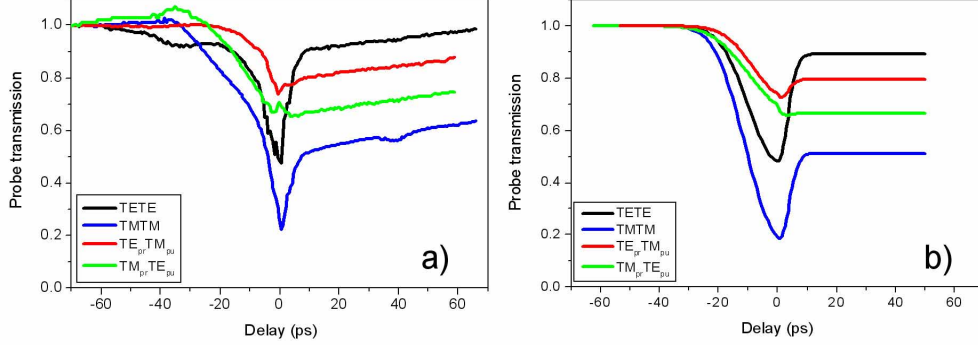


Fig. 2. Experimental a) and simulated b) probe transmission for the co- and cross-polarized inputs. The pump and probe pulse energies are 24fJ and 12fJ, respectively.

The fast recovery component is usually attributed to SHB and CH effects [10]. It is most evident in the co-polarized cases. The fast recovery dominates the probe transmission for the TETE case, where only a small level of slow gain recovery remains. A fast component is also evident for the TMTM case but here there is a greater contribution of the slow gain recovery. The intraband effects are only significant in the co-polarized cases. The slow recovery is observed after  $C$ .

In Fig. 2(b), the simulation results of the transmission of the probe signal in co- and cross-polarization configurations are shown for the same energy values as used in the experiment. The pulse full width at half-maximum is set at 2.5ps and the parameters used are listed in Table I. The value of  $E_{sat}$  is adjusted until the level of the slow gain recovery at  $C$  matches the experimentally observed value. The value of  $\epsilon$  is then adjusted until the simulated value of the total gain compression matches the experimental data. Comparison of Fig. 2(a) and 2(b) shows that the proposed model can simulate well the experimental observations. In the cases of co-polarized states, the gain recovery is faster for the TETE configuration than for the TMTM. In the cases of cross-polarized states, the gain recovery is drastically reduced.

By fitting the experimental results with this computational model, it is possible to determine the polarization dependence of  $\epsilon$ . The extracted values are summarized as:  $\epsilon^{TETE} = 8 \times 10^{-23} m^3$ ,  $\epsilon^{TE_p TM_{pu}} = 1 \times 10^{-23} m^3$ ,  $\epsilon^{TM_{pr} TE_{pu}} = 1.6 \times 10^{-23} m^3$  and  $\epsilon^{TMTM} = 25 \times 10^{-23} m^3$ . These values are within the range of values quoted in literature [1-4].  $\epsilon$  for co-polarized pump and probe pulses is larger than for cross-polarized pump and probe pulses and reflects the fact the contribution of the intraband effects are larger for co-polarized signals than for cross-polarized ones. The polarization dependence of  $\epsilon$  reflects the polarization dependence of the intraband gain recovery mechanisms.

#### 4.2 Effect of the pump signal energy

By varying the energy of the pump pulse, it is possible to investigate the influence of the pump pulse energy on the intraband contribution of the gain recovery. Fig. 3 shows the power dependence of  $\epsilon$  for the four polarization combinations. It can be seen that  $\epsilon$  decreases with increasing pump pulse energy for all pump-probe polarization configurations. Regarding the co-polarization cases, stronger energy dependence can be observed and the value of  $\epsilon$  is approximately 10 times greater. When the pump and probe polarizations are co-linear the compression of the gain experienced by the probe signal is larger as the pump signal is depleting the carriers contributing to the transmission of the probe signal. When the pump and the probe polarizations are crossed, the carriers contributing to the transmission of the probe are less affected by the pump signal. Such an effect would be most evident when pumping and probing at the same wavelength, as in this experimental study.

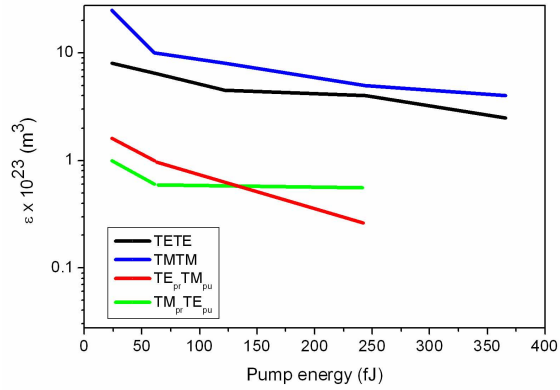


Fig. 3. Nonlinear gain compression correction factor as a function of the input pump energy for the four states of polarization of injected signals. Probe energy: 12 fJ.

## 5. Conclusion

A contra-propagation pump-probe experiment was used to investigate the polarization dependence of gain dynamics in an SOA device. The advantages of this set-up are multiple, as it allows for any combination of pump and probe polarizations and wavelengths, including co-polarized resonant pump and probe signals. The results show a clear dependence of the fast gain recovery with the polarization and energy of the injected signals. Furthermore a phenomenological model based on travelling waves in SOA has been developed. This model takes into account the intraband effects by introducing a nonlinear gain compression factor. Good agreement between the experimental results and the simulation has been obtained. While the model does not take account of the slow gain recovery, it is sufficient to investigate the polarization dependence of intraband gain recovery mechanisms. The dependence of the nonlinear gain compression correction factor  $\varepsilon$  has been studied and has shown a large influence of the polarization on this parameter which may explain discrepancy observed in the estimated values of  $\varepsilon$  in past references. The polarization dependence of  $\varepsilon$  reflects the polarization dependence of intraband gain recovery mechanisms.

## Acknowledgement

This work is supported by Commercialisation Fund Technology Development programme from Enterprise Ireland, project CFTD/06/IT/332.